Computational and Experimental Research in Materials and Renewable Energy (CERiMRE)
Volume 8, Issue 2, page 175-206
eISSN : 2747-173X

Submitted : September 11, 2025
Accepted : November 12, 2025
Online : November 28, 2025
DOI : 10.19184/cerimre.v8i2.4

Energy Recovery from Corn Straw via Batch Anaerobic Digestion: Experimental and Simulation Study Using Rumen Inoculum

Kabama Kasombo[1,3,4,a], Tuba Mbemba[1], Mabengi Kipupa[1,3], Kasongo Kanyinda[1,3], Buetham Mbidika[1], Masuama Rossy[1], Mapepe Nyamaha[1], Sunda Makuba[2], Kapanga Muamba[3,4], and Tshimanga Muamba[3,4]

[1]Faculty of Oil, Gas and Renewable Energies, University of Kinshasa, Democratic Republic of the Congo

[2]Faculty of Sciences and Technology, University of Kinshasa, Democratic Republic of the Congo

[3]Regional School of Water (ERE), University of Kinshasa, Democratic Republic of the Congo

[4]Congo Basin Water Resources Research Center (CRREBaC), Democratic Republic of the Congo

[a]email: napoleon.kabama@unikin.ac.cd

Abstract. *This study examines the experimental and simulation-based performance of batch anaerobic bioreactors used for the biomethanization of corn straw inoculated with rumen juice from the Masina slaughterhouse. The objective was to evaluate the substrate inoculum interaction under discontinuous operating conditions. Volumetric, gravimetric, and electrometric methods, along with the principle of communicating vessels, were used to monitor the bioconversion process. A two-phase anaerobic digestion model was developed to simulate the evolution of key parameters such as substrate concentration, microbial activity, and methane production over time. Model outputs were compared with experimental results to validate its accuracy and gain insight into degradation dynamics. Two inoculum conditioning strategies were tested to assess their effect on enzymatic activity and methane yield. Preconditioned (non-fresh) rumen juice, combined with a high organic loading rate, significantly improved the hydrolysis of lignocellulosic biomass, leading to faster degradation and enhanced methane productivity. The approach relied on simple, low-cost techniques and delivered promising results. A significant volume of methane was generated after 28 days of digestion, confirming the efficiency of the selected process conditions. These findings highlight the potential of anaerobic digestion for valorizing agricultural waste into bioenergy, particularly in decentralized, resource constrained contexts.The cumulative methane productions for the experimental digesters I, II, III, and IV were 330 mL, 412 mL, 153 mL, and 197 mL respectively, while the simulation predicted a maximum methane production rate of 0.375 L/day at an initial dissolved glucose concentration of 5 $g \cdot L^{-1}$. These results emphasize the importance of developing local and sustainable biogas production processes from organic waste, thereby contributing to energy transition, greenhouse gas reduction, and the promotion of a circular economy within the renewable energy sector.*

Keywords: Anaerobic Digestion, Corn Straw, Rumen Inoculum, Biogas Production, Bioreactor Modeling

Computational and Experimental Research in Materials and Renewable Energy (CERiMRE)
Volume 8, Issue 2, page 175-206
eISSN : 2747-173X

Submitted : September 11, 2025
Accepted : November 12, 2025
Online : November 28, 2025
DOI : 10.19184/cerimre.v8i2.4

Introduction

Climate change remains one of the most urgent and complex challenges of the 21st century [1], with severe implications for ecosystems, human health, food security, and global economies. The continued reliance on fossil fuels coal, oil, and natural gas as the primary energy sources has led to a dramatic increase in greenhouse gas (GHG) emissions [2], particularly carbon dioxide (CO_2), which are the main drivers of global warming and environmental degradation [1]. The consequences include rising sea levels, more frequent natural disasters, and the loss of biodiversity [3]. The energy sector alone accounts for nearly 70% of global GHG emissions, making it a key focus of climate mitigation strategies [1]. In response, the scientific community and policymakers are accelerating the transition toward renewable and low-carbon energy sources, such as solar, wind, hydroelectricity, geothermal energy, and biomass [4]. The global demand for renewable energy is increasing as countries work to transition from fossil fuels in order to combat climate change and ensure long-term energy security. Renewable energy sources, are naturally replenished and offer sustainable, environmentally friendly alternatives to conventional energy sources [5]. Among these, biomass stands out due to its abundance, renewability, and capacity for decentralized energy production, especially in rural and low-income regions [6].

Lignocellulosic biomass is an abundant and renewable resource originating from plants, and its major composition is polysaccharides (cellulose and hemicellulose) added to lignin (an aromatic polymer). It is viewed as the only sustainable source of organic carbon on Earth with net-zero carbon emission; thus, it has no adverse environmental effects. The production of lignocellulosic biomass is quick, and it has a lower cost than other types of resource feedstock [7]. Recent research has emphasized the role of lignocellulosic biomass derived from agricultural residues like corn straw, rice husks, or sugarcane bagasse as a valuable feedstock for anaerobic digestion [6]–[8]. This biological process, also known as biomethanization, involves the microbial degradation of organic matter under anaerobic conditions, producing biogas, a mixture primarily composed of methane and carbon dioxide [7].

Despite its potential, lignocellulosic biomass is recalcitrant, requiring pre-treatment or microbial enhancement to improve hydrolysis and biogas yield [9]. Several strategies have been explored, such as physical, chemical, enzymatic, or biological conditioning, but no universal solution has been adopted. One promising approach involves the use of rumen juice, a natural inoculum rich in cellulolytic and methanogenic microorganisms, which has shown encouraging results in improving methane production from fibrous materials [10]–[12].

However, existing studies offer divergent conclusions regarding the effectiveness of rumen inoculation. Some report significant increases in methane yield and faster degradation rates [11], while others observe limited or inconsistent results depending on substrate composition, reactor configuration, and inoculum freshness [13], [14]. These discrepancies underline the need for further experimental validation and mechanistic modeling to better understand the underlying dynamics.

While previous studies have explored anaerobic digestion of lignocellulosic residues using various co-digestion or pretreatment approaches like [10], [13], this work distinguishes itself by combining experimental and simulation based analyses of batch anaerobic bioreactors inoculated with rumen juice sourced from the Masina slaughterhouse. Unlike most recent research focusing on laboratory-cultured inoculate or continuous systems, this study investigates the use of a naturally

Computational and Experimental Research in Materials and Renewable Energy (CERiMRE)
Volume 8, Issue 2, page 175-206
eISSN : 2747-173X

Submitted : September 11, 2025
Accepted : November 12, 2025
Online : November 28, 2025
DOI : 10.19184/cerimre.v8i2.4

enriched microbial consortium under discontinuous (batch) conditions, emphasizing simplicity, low cost, and local applicability. Moreover, the integration of a two-phase anaerobic digestion model provides a novel quantitative interpretation of substrate inoculum interactions and degradation kinetics. By validating the model with experimental data, this research offers new insights into how inoculum conditioning and organic loading affect methane yield, particularly in decentralized and resource-limited context.

In this study, corn straw, an abundant agricultural waste product often discarded in agro-industrial systems, is used as the substrate for biomethanization. The main objective is to evaluate the performance of batch anaerobic digestion of corn straw inoculated with rumen juice, under controlled laboratory conditions. The study combines experimental investigations with the development of a two-phase kinetic model, simulating the key steps of anaerobic digestion: hydrolysis, acidogenesis, acetogenesis, and methanogenesis.

By integrating empirical data with simulation results, this research aims to assess the effect of inoculum conditioning on methane productivity, optimize organic loading strategies, and validate the model for potential application in continuous fermentation systems. MATLAB® is employed to numerically solve and calibrate the model equations.

Therefore, the study focuses on the anaerobic digestion of corn straw as a promising pathway for converting abundant agricultural residues into renewable bioenergy. This approach not only addresses the environmental challenges associated with agricultural waste management but also enhances climate resilience by reducing greenhouse gas emissions and promoting sustainable resource cycles. Furthermore, it supports local energy autonomy and rural development. By optimizing the digestion process and exploring bio-augmentation strategies, the research aims to increase biogas yield and improve the overall efficiency of biomass utilization, thereby contributing to the goals of renewable energy expansion, circular economy, and climate adaptation.

Theoretical Background

Anaerobic digestion (AD) is a complex biochemical process in which a consortium of microorganisms converts organic matter into biogas under oxygen-free conditions. The generated biogas mainly consists of methane (CH_4) and carbon dioxide (CO_2), representing a renewable and environmentally friendly energy source [12], [15]. The AD process involves four main stages: hydrolysis [16], acidogenesis, acetogenesis, and methanogenesis [17], [18]. Each phase is mediated by specific microbial communities and strongly influenced by environmental factors such as temperature, pH, substrate composition, and the carbon-to-nitrogen (C/N) ratio.

In the hydrolysis step, complex organic polymers cellulose, hemicellulose, and lignin are broken down into monomers such as sugars, amino acids, and fatty acids. This stage often limits the overall rate of biogas production, particularly when lignocellulosic materials like corn straw are used as substrates [19]. During acidogenesis, these monomers are converted into volatile fatty acids (VFAs), alcohols, CO_2, and H_2, which are then transformed into acetate and H_2 in the acetogenesis phase. Finally, methanogenic archaea utilize acetate and hydrogen to produce methane, the main energy component of biogas.

Corn straw is one of the most abundant agricultural residues in the world, rich in lignocellulosic biomass (cellulose ≈ 35–40%, hemicellulose ≈ 25–30%, and lignin ≈ 15–20%) [9]. However, its

Computational and Experimental Research in Materials and Renewable Energy (CERiMRE)
Volume 8, Issue 2, page 175-206
eISSN : 2747-173X

Submitted : September 11, 2025
Accepted : November 12, 2025
Online : November 28, 2025
DOI : 10.19184/cerimre.v8i2.4

rigid lignin cellulose structure makes it resistant to microbial attack, thus requiring pretreatment or bio-augmentation to enhance degradability and methane yield [20]. The use of rumen inoculum, derived from ruminant stomachs, introduces a highly efficient microbial consortium containing cellulolytic bacteria and methanogenic archaea that can accelerate fiber degradation and improve process kinetics [21].

In this context, batch anaerobic digestion provides a simple yet effective experimental configuration to evaluate process kinetics and cumulative biogas production. Batch systems allow controlled observation of substrate degradation dynamics, microbial adaptation, and biogas yield under specific inoculum substrate ratios [13]. To quantitatively describe and predict system performance, mathematical modeling plays a central role. In this study, a biphasic model was applied to represent the dual dynamics of acidogenic and methanogenic phases. Unlike single-phase first-order kinetic models, the biphasic model assumes that the AD process occurs in two distinct yet overlapping stages with different rate constants (k_1 and k_2). The first phase (acidogenesis) represents the rapid degradation of readily biodegradable compounds, while the second (methanogenesis) models the slower conversion of intermediates into methane [22]. This approach provides a more accurate description of the cumulative methane yield curve, especially when treating heterogeneous substrates such as corn straw.

The combination of experimental batch tests and biphasic kinetic simulation enables a deeper understanding of microbial dynamics and substrate utilization efficiency. Such integrated analysis contributes to optimizing digestion conditions and improving the overall performance of anaerobic systems for sustainable energy recovery, waste reduction, and climate resilience. **Figure 1** shows a simplified schematic of the batch anaerobic digestion process using corn straw as the primary substrate for biogas and methane (CH_4) production.

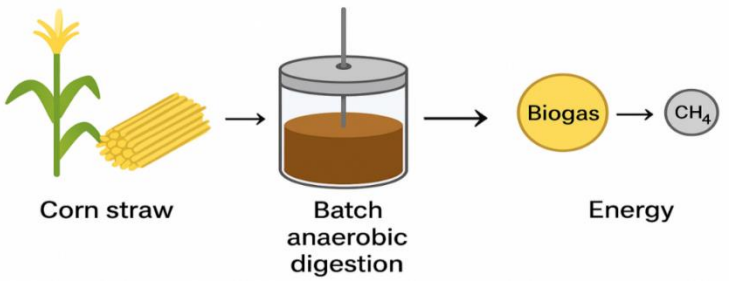

Figure 1. Simplified diagram of the batch anaerobic digestion process using corn straw as substrate for biogas and methane (CH_4) production

Materials and Methods

The implementation of this research relied on a combination of documentary research, experimental analysis, and numerical simulation using software tools such as Microsoft Excel 2021 for data management and MATLAB R2019b for model computation.

Biphasic Simulation of Anaerobic Bioreactors

A mathematical model is a simplified representation of a real system, expressed through a set of equations that reflect the essential behaviors of that system [18], [20]. In this study, the model

Computational and Experimental Research in Materials and Renewable Energy (CERiMRE)
Volume 8, Issue 2, page 175-206
eISSN : 2747-173X

Submitted : September 11, 2025
Accepted : November 12, 2025
Online : November 28, 2025
DOI : 10.19184/cerimre.v8i2.4

focuses on key physical and operational parameters influencing anaerobic digestion, such as temperature, hydraulic retention time (HRT), and reactor volume.

The complexity of the model is directly related to the number of microbial populations considered. In order to simplify without compromising critical mechanisms, it is assumed that the microbial community can be grouped into two main functional groups: acidogenic and methanogenic bacteria. Anaerobic digestion is thus represented as a two-phase system: 1) in the acidogenesis phase, fermentative bacteria degrade the organic substrate into volatile fatty acids (VFAs) and carbon dioxide (CO_2), and 2) in the methanogenesis phase, methanogenic archaea convert VFAs into methane (CH_4) and CO_2 [19]. This biphasic approach provides foundational insight into both biochemical dynamics (e.g., microbial growth), chemical indicators (e.g., pH, ammonia concentration), and the quantity of biogas produced throughout the digestion process [23].

The original form of this model was developed for simulating anaerobic digestion of organic waste in a continuous stirred tank reactor (CSTR) operating at mesophilic temperature (36 ºC) [22], [23], and accounted for ammonia and pH inhibition effects [24]. In its original application, the model simulated the digestion of pig slurry and wastewater treatment sludge, often leading to high ammonia concentrations in biogas [25]. High total nitrogen and free nitrogen of poultry manure is a serious challenge for the microbial communities during the anaerobic digestion process. Theoretically speaking, increasing OLR should result in higher methane production but practically, due to elevated concentration of total and free ammonia, ammonia inhibition occurred resulting in lower methane production [26]. In the context of this study, the model has been adapted to simulate batch digestion of corn straw mixed with bovine rumen juice. The ammonia concentration in the system is considered negligible, which simplifies inhibition modeling and better reflects the characteristics of the substrate-inoculum matrix used in this experiment.

Different Reactor Configuration

Anaerobic digestion systems are characterized by slow microbial growth, particularly for methanogenic archaea, which requires a longer hydraulic retention time (HRT) compared to aerobic systems. However, this also results in a more stable equilibrium within the microbial consortia [25]. Several reactor configurations have been developed to improve retention, enhance microbial contact, and optimize gas production [27]. These include: batch reactors, completely stirred tank reactors (CSTR), upflow anaerobic sludge blanket (UASB) reactors, and fixed-film reactors. The configuration selected for this study is a batch stirred reactor, due to its simplicity, low cost, and appropriateness for laboratory-scale trials. An illustrative overview of common anaerobic reactor types is provided in **Figure 2**.

When a bacterial inoculum is introduced into a closed system containing a non-renewed nutrient medium, the dynamics of microbial biomass (X) over time follow a characteristic sigmoid growth curve as illustrated in **Figure 2** [25], [28]. This curve is typically divided into six distinct phases, each representing a stage in the microbial adaptation and proliferation process:

1) Phase I – Lag phase (latency): during this initial phase, cells adapt to the new environment. Although metabolic activity begins, no significant growth occurs as the microorganisms are adjusting their enzymatic systems to the available substrates [29].

Computational and Experimental Research in Materials and Renewable Energy (CERiMRE)
Volume 8, Issue 2, page 175-206
eISSN : 2747-173X

Submitted : September 11, 2025
Accepted : November 12, 2025
Online : November 28, 2025
DOI : 10.19184/cerimre.v8i2.4

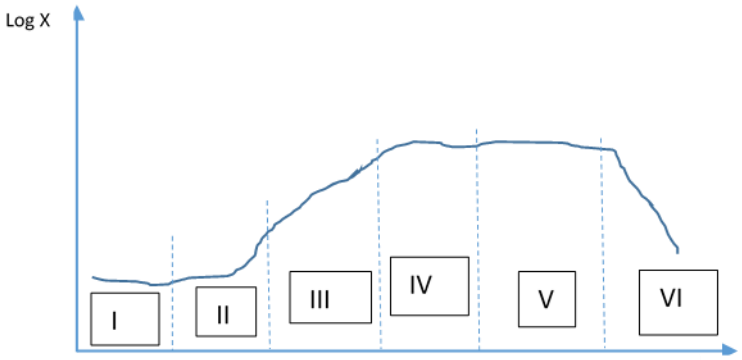

Figure 2. Different stages of microbial growth in batch culture (discontinuous feeding) [28]

2) Phase II – Acceleration phase: enzymatic systems become progressively activated, and the growth rate increases. This is considered a transition zone toward exponential growth, still influenced by nutritional and physiological adaptation.

3) Phase III – Exponential (log) growth phase: microorganisms divide at their maximum specific growth rate (μ_{max}) under the given environmental conditions. Substrate availability is high, and growth is only limited by the intrinsic kinetics of the cells [30].

4) Phase IV – Deceleration phase: the growth rate decreases due to the progressive depletion of nutrients and accumulation of inhibitory metabolic by-products such as VFAs or ammonia.

5) Phase V – Stationary phase: cell division ceases, and a dynamic equilibrium is reached between cell proliferation and cell death. Nutrients are exhausted, and inhibitory compounds reach critical concentrations. Secondary metabolism may dominate during this phase.

6) Phase VI – Death or decline phase: the cell population enters a state of net decline as lysis or death exceeds cell formation. Energy reserves are depleted, and toxic conditions may prevail.

Phases I and II are commonly grouped under the "adaptation phase", which reflects the influence of the culture medium on bacterial physiology. This stage involves complex molecular regulation, including induction of specific enzymes, genetic regulation, and transport system activation to adapt to the new medium [31].

In phase III, the increase in growth in X bacterial biomass is proportional to the time and concentration in bacteria present:

$$dX = \mu \cdot X dt \quad (1)$$

Where μ is called growth rate, of dimension t^{-1}.

During phase III, growth at a constant μ rate is ensured by the consumption of the nutrient substrate S (expressed in concentration). This is called growth yield:

Computational and Experimental Research in Materials and Renewable Energy (CERiMRE)
Volume 8, Issue 2, page 175-206
eISSN : 2747-173X

Submitted : September 11, 2025
Accepted : November 12, 2025
Online : November 28, 2025
DOI : 10.19184/cerimre.v8i2.4

$$Y = \frac{dX}{dS} \tag{2}$$

Experience shows that Y, which uniquely characterizes the middle species pair, remains constant during this phase. The amount of substrate consumed is proportional to the time and quantity of biomass:

$$dS = q_s \cdot X dt \tag{3}$$

q_s is called the metabolite coefficient for a given substrate, of dimension t^{-1}.

Given the previous definitions, we have:

$$q_s = \frac{\mu}{Y} \tag{4}$$

The exponential phase continues as long as there is no factor limiting growth. A limiting factor, a priori obvious, is the volume of the fermentor. If it were to play alone, theoretically a maximum microbial density of 1011 cells/mL could be observed. In fact, we rarely exceed 109 in the best conditions because the real limiting factors are on the one hand the quantities of nutrients available, on the other the appearance of bacteriostatic bacterial metabolites (i.e. inhibiting the growth of bacteria without killing them) or even bactericides. The intervention of the latter and the depletion of nutrients characterize phase IV. Since all growth reactions are enzymatic in nature, if we assimilate a biomass to a coherent set of enzyme sites, we obtain, thanks to a reasoning similar to the one that allows to establish the Michaelis-Menten equation for enzymes, a transposed form of the latter for microbial growth [25]

Degradation kinetics are described by a variety of mathematical expressions of increasing complexity as attempts to integrate the many variables affecting the disappearance of organic matter (MO). One of the most commonly used models is kinetics of order 1. The speed of degradation is proportional to the concentration of a single reactive: the MO. This model considers MO as a homogeneous, i.e. mono-molecular, substance with a constant degradation rate equal to □ [32]:

$$\frac{d[s]}{dt} = -k[s] \tag{5}$$

which is integrated into:

$$e^{-kt} = \frac{[s]}{[S_0]} \; or \; [s] = [S_0]\, e^{-kt} \tag{6}$$

with:

k = degradation or hydrolysis constant (j^{-1})

t = duration of degradation (j)

$[S_0]$ = initial substrate concentration ($mol.L^{-1}$)

$[s]$ = substrate concentration in time ($mol.L^{-1}$)

Computational and Experimental Research in Materials and Renewable Energy (CERiMRE)
Volume 8, Issue 2, page 175-206
eISSN : 2747-173X

Submitted : September 11, 2025
Accepted : November 12, 2025
Online : November 28, 2025
DOI : 10.19184/cerimre.v8i2.4

This vision of degradation according to kinetics of order 1 comes from the fact that the limiting step is the breakdown of polymers into small soluble molecules (amines, monosaccharides, fatty acids). The fastest reaction imposes its speed on degradation; here we find the idea of "master reaction" dictating its speed to the whole of a system, advanced by Jacques Monod for enzymatic reactions.

Recent kinetic modeling studies have validated these relationships in anaerobic digestion contexts. For instance, [24] applied Monod-type models to describe microbial growth and substrate degradation in anaerobic reactors using lignocellulosic feedstocks. [21] estimated $\mu_{\max}$ (~0.098 h^{-1}) and the half-saturation constant □[□] (~1.2 × 10^8 mg/L) for mixed organic wastes using Monod kinetics.

Despite the heterogeneity of aquatic microbial populations, it appears that the rate of use of a substrate by microbic biomass obeyes a Michael kinetics:

$$\frac{d[s]}{dt} = -\frac{v_{max\,.\,[S]}}{k_m + [S]} \tag{7}$$

with v_{max} = maximum reaction speed ($g.L^{-1}.j^{-1}$)

$[S]$ = substrate quantity ($g.L^{-1}$)

k_m = saturation or Michaelis constant ($k_m = [S]$ for $V = v_{max}/2$) ($g.L^{-1}$)

The maximum reaction speed is the theoretical initial speed of an enzymatic reaction for an infinite substrat concentration.

Hess 2007, gives the hydrolysis constants (k ≈ 0.205 – 0.285 d^{-1}) for thermophilic anaerobic digestion of duckweed biomass, aligning with rates typically observed in efficient systems [28].

Specific biomass growth rates

The model chosen to express the specific growth rate of the acidogenic bacterial community is as follows [32]:

$$\mu_a = \frac{\mu_{amax}}{1 + \frac{K_{x_a}}{S} + \frac{A_h}{K_{ix_a}}} \tag{8}$$

in which,

μ_{amax} = acidogenic biomass specific growth rate (j^{-1})

K_{x_a} = acidogenic bacterial growth saturation constant ($g.L^{-1}$)

S = substrate glucose equivalent concentration ($g.L^{-1}$)

K_{ix_a} = acetic acid inhibition constant on acidogenic bacterial growth ($g.L^{-1}$).

A_h = non-ionized acetic acid concentration ($g.L^{-1}$) given by:

$$A_h = \frac{A.H^+}{K_c} \tag{9}$$

Computational and Experimental Research in Materials and Renewable Energy (CERiMRE)
Volume 8, Issue 2, page 175-206
eISSN : 2747-173X

Submitted : September 11, 2025
Accepted : November 12, 2025
Online : November 28, 2025
DOI : 10.19184/cerimre.v8i2.4

where, $\square_h$ is the total concentration of acetic acid, H^+ is that of hydrogen ion, and K_c is the dissociation constant for acetic acid at 35 ºC, equal to $1{,}728 \times 10^{-5}$. As for the methanogenic bacterial population, its specific growth rate is governed by the Haldane model, neglecting the concentration of ammonia:

$$\mu_m = \frac{\mu_{mmax}}{1 + \frac{K_{X_m}}{A_h} + \frac{A_h}{K_{iX_m}}} \tag{10}$$

where,

μ_{mmax} = methanogenic biomass specific growth rate (j^{-1})

K_{X_m} = methanogenic growth saturation constant ($g.L^{-1}$)

K_{iX_m}= acetic acid inhibition constant on the growth of methanogenic bacteria ($g.L^{-1}$)

System mass balance

Variation in acidogenic biomass

The variation of the acidogenic biomass X_a over time is governed by the following equation [32]:

$$\frac{dX_a}{dt} = \mu_a X_a - K_{da} X_a + X_a D \tag{11}$$

with D Dilution rate which, in the case of continuous operation of the digester, is given by the following relationship:

$$D = \frac{Q_V}{V_{liq}} \tag{12}$$

in which, Q_V designates the inlet and outlet volume flow of the substrate ($L.j^{-1}$) and V_{liq} is the volume of the liquid phase. Or $D = 0$, for a batch reactor, the equation then becomes:

$$\frac{dX_a}{dt} = \mu_a X_a - K_{da} X_a \tag{13}$$

Variation of the acidogenic biomass, where K_{da} (j^{-1}) and μ_a (j^{-1}), respectively designate the lysis rate and the specific growth rate of this acid-producing population.

Variation in methanogenic biomass

In the same way, the evolution of the methanogenic population $\boldsymbol{X_m}$ is governed by a mass balance equation with a form similar to the previous one [21]:

$$\frac{dS}{dt} = D.\left(S_{inf} - S\right) - \frac{\mu_a . X_a}{Y_a} + \frac{\mu_a . X_a}{Y_{so}} \tag{14}$$

or $D = 0$

$$\frac{dX_m}{dt} = \mu_m X_m - K_{dm} X_m \tag{15}$$

Computational and Experimental Research in Materials and Renewable Energy (CERiMRE)
Volume 8, Issue 2, page 175-206
eISSN : 2747-173X

Submitted : September 11, 2025
Accepted : November 12, 2025
Online : November 28, 2025
DOI : 10.19184/cerimre.v8i2.4

With K_{dm} (j^{-1}) and μ_m (j^{-1}), respectively the lysis rate and the specific growth rate of this bacterial community.

Variation of the starting complex substrate

This model considers that the initial substrate is composed of glucose. Thus, the mass balance equation relating to the evolution of the equivalent glucose concentration of the substrate is written as follows [21]:

$$\frac{dS}{dt} = D.\left(S_{inf} - S\right) - \frac{\mu_a.X_a}{Y_a} + \frac{\mu_a.X_a}{Y_{so}} \tag{16}$$

when D = 0, we will have:

$$\frac{dS}{dt} = -\frac{\mu_a.X_a}{Y_{va}} + \frac{\mu_a.X_a}{Y_{so}} \tag{17}$$

where,

Y_{va} = yield coefficient linked to the degradation of the complex substrate caused by acidogenic bacteria X_a (g.g^{-1})

Y_{so} = yield coefficient linked to the formation of soluble organic matter (g.g^{-1})

In the right hand side of the equation, the second term $\frac{\mu_a.X_a}{Y_{va}}$ represents the use of glucose by acidogenic bacteria in their metabolism and the third term $\frac{\mu_a.X_a}{Y_{so}}$ represents the production of glucose from volatile materials.

Acetic acid variation

The second type of substrate consists mainly of acetic acid A serving as food for the methanogenic bacterial population X_m. The evolution of the total concentration of this volatile fatty acid is governed by the following equation [33]:

$$\frac{dA}{dt} = D.\left(A_{inf} - A\right) + \frac{\mu_a.X_a}{Y_{va}} - \frac{\mu_m.X_m}{Y_m} \tag{18}$$

by eliminating D, the equation will become:

$$\frac{dA}{dt} = \frac{\mu_a.X_a}{Y_{va}} - \frac{\mu_m.X_m}{Y_m} \tag{19}$$

in which:

A_{inf} = concentration of acetic acid in the influent (g.L^{-1})

Y_{va} = yield coefficient of the conversion of the substrate into acetic acid by the acidogenic biomass (g.g^{-1})

Y_m = Yield coefficient linked to the consumption of acetic acid by methanogenic biomass (g.g^{-1})

Computational and Experimental Research in Materials and Renewable Energy (CERiMRE)
Volume 8, Issue 2, page 175-206
eISSN : 2747-173X

Submitted : September 11, 2025
Accepted : November 12, 2025
Online : November 28, 2025
DOI : 10.19184/cerimre.v8i2.4

Methane production rate

The rate of methane production according to the model of Moletta et al is linked to the concentration of non-ionized acid by the relationship [33]–[35]:

$$v_{PCH_4} = \frac{dCH_4}{dt} = V_{mmax}.X_m\left(\frac{A_h}{A_h + K_m}\right)\left(\frac{K_{im}}{K_{im} + A_h}\right) \quad (20)$$

with:

V_{mmax} = maximum rate of CH_4 production by methanogenic bacteria ($g.g^{1}.j^{1}$)

K_m = saturation constant of methane production ($g.L^{-1}$)

K_{im} = inhibition constant of acetic acid on production of CH_4 ($g.L^{-1}$)

Carbon dioxide production rate

Establishing the mass balance relating to the concentration of carbon dioxide requires knowledge of the different production and consumption rates of this gaseous component, namely [36], [37]:

1) Rate of CO_2 production by the action of methanogenic biomass $(\mathrm{R_M})$

This speed is directly linked to the growth speed of methanogenic bacteria $\mu_m.X_m$ as follows:

$$R_M = \frac{\mu_m.X_m.Y_{CO_{2m}}}{M_x} \quad (21)$$

where $Y_{CO_{2m}}$ ($g.g^{-1}$) represents the efficiency coefficient of CO_2 production by methanogenic biomasses whose molar mass M_x is assumed to be equal to 113 $g.mol^{-1}$ [21].

2) Rate of formation of CO_2 linked to the production of acetic acid $(\mathrm{R_{AC}})$

Carbon dioxide can be formed from HCO_3^- bicarbonates during the production of acetic acid. The variation of CO_2 resulting from this transformation is given by:

$$R_{AC} = \frac{1}{M_a}\frac{dA}{dt} \quad (22)$$

M_a being the mole fraction of acetic acid ($g.mol^{-1}$).

3) Rate of formation of CO_2 by the action of acidogenic biomasses $(\mathrm{R_{AF}})$

Analogous to the case of RM, this rate of CO_2production is linked to the rate of growth of the acidogenic bacterial community $\mu_a.X_a$ a such that [38]:

$$R_{AF} = \frac{\mu_a.X_a.Y_{CO_{2a}}}{M_x} \quad (23)$$

with $Y_{CO_{2a}}$ ($g.g^{-1}$) is the efficiency coefficient of CO_2 formation due to the activities of acidogenic biomasses.

Computational and Experimental Research in Materials and Renewable Energy (CERiMRE)
Volume 8, Issue 2, page 175-206
eISSN : 2747-173X

Submitted : September 11, 2025
Accepted : November 12, 2025
Online : November 28, 2025
DOI : 10.19184/cerimre.v8i2.4

4) Rate of CO_2 consumption due to the release of the cation other than H^+ (R_Z)

The degradation of the complex primary substrate to form HCO_3^- bicarbonates causes a release of cations. By representing the cation by □ (L^{-1}), the rate of CO_2 consumption relative to the resulting reactions and the rate of variation of □ are equivalent [9]:

$$R_Z = \frac{dZ}{dt} \tag{24}$$

Flow rates of biogas and its components

The total biogas flow rate Q ($L.j^{-1}$) is the sum of the flow rates of its main components, namely methane and carbon dioxide [21]:

$$Q = Q_{CH_4} + Q_{CO_2} \tag{25}$$

$$Q_{CO_2} = -S_V.V_{rec}.R_T \tag{26}$$

$$Q_{CH_4} = (S_V.V_{rec})\left(\frac{1}{M_{CH_4}}\right)(\mu_m X_m Y_{CH_4}) \tag{27}$$

With S_V = standard volume (equal to 22.4 $L.mol^{-1}$), M_{CH_4} = molar mass of methane, Y_{CH_4} = coefficient of efficiency of methane production

Calculation of pH

For a pH between 5 and 8, the concentration of bicarbonate is expressed as follows [26], [38], [39]:

$$HCO_3^- = Z^+ - \frac{A_h}{M_a} \tag{28}$$

The hydrogen ion (H^+) is given by:

$$H^+ = \frac{K_{CO_2}.CO_2}{HCO_3^-} \tag{29}$$

where K_{CO_2} is the ionization constant of CO_2 (equal to 4.72×10^{-7} at 35 ºC).

The pH can be obtained as follows:

$$pH = -log(H^+) \tag{30}$$

Calibrated process parameters

The parameter intervals were derived from a model reported in the literature, but the actual parameter estimates were determined based on our own experimental data and the specific context of our biphasic modeling study. The calibrated process parameters are shown in **Table 1** (a, b, and c). **Table 1 (c)** presents the key operating and design parameters of the digester system

Computational and Experimental Research in Materials and Renewable Energy (CERiMRE)
Volume 8, Issue 2, page 175-206
eISSN : 2747-173X

Submitted : September 11, 2025
Accepted : November 12, 2025
Online : November 28, 2025
DOI : 10.19184/cerimre.v8i2.4

used in this study. These parameters are critical for understanding the overall performance and efficiency of the anaerobic digestion process.

Table 1. Calibrated process kinetics parameters

Parameter	Range of Variation	Nominal Value
(a) Process Kinetics Parameters		
K_{da}	[0 ; 1]	0.150
μ_{amax}	[0 ; 1]	0.350
K_{x_a}	[0 ; 1]	0.950
K_{ix_a}	[0 ; 1]	0.010
K_{dm}	[0 ; 1]	0.060
μ_{mmax}	[0 ; 1]	0.950
K_{x_m}	[0 ; 1]	0.015
K_{im}	[0 ; 1]	0.015
K_{ix_m}	[0 ; 1]	0.010
(b) Process Productivity Parameters		
Y_a	[0 ; 1]	0.188
Y_{cat}	[0 ; 1]	0.150
$Y_{CO_{2m}}$	[0 ; 30]	18.000
Y_{so}	[0 ; 1]	0.950
Y_{va}	[0 ; 1]	0.750
V_{mmax}	[0 ; 1]	0.100
Y_{CH_4}	[0 ; 30]	10.000
$\boldsymbol{Y_{co_{2m}}}$	[0 ; 30]	12.500
Y_m	[0 ; 1]	0.080
(c) Digester Parameters		
K_{ia}	[0 ; 12]	1
V_{rec}	[0 ; 1]	0.5

Validation process

The predictive performance of the developed model for anaerobic digestion (biomethanation) was evaluated using four statistical indicators: the coefficient of determination (R^2), the root mean square error (RMSE), the mean absolute error (MAE), and the Pearson correlation coefficient (r) [40], [41]. These indicators quantify the level of agreement between the simulated results and the experimental measurements of biogas or methane production. These indicators were computed as follows:

$$RMSE = \sqrt{\left((1/N) + \sum(\hat{y}_i - y_i)^2\right)}, \quad R^2 = 1 - \frac{\sum(\hat{y}_i - y_i)^2}{\sum(y_i - \bar{y})^2} \tag{31}$$

$$MAE = \left(\frac{1}{N}\right) \times \sum[\hat{y}_i - y_i], \quad r = \frac{\sum(y_i - \bar{y}_i)(\hat{y}_i - \hat{y})}{\sqrt{(\sum(y_i - \bar{y})^2 \times \sum(\hat{y}_i - \hat{y})^2)}} \tag{32}$$

where y_i and $\hat{y}_i$ denote the experimental and simulated values, respectively, $\bar{y}$ and $\hat{y}$ are their means, and N is the number of data points.

Computational and Experimental Research in Materials and Renewable Energy (CERiMRE)
Volume 8, Issue 2, page 175-206
eISSN : 2747-173X

Submitted : September 11, 2025
Accepted : November 12, 2025
Online : November 28, 2025
DOI : 10.19184/cerimre.v8i2.4

RMSE measures the average magnitude of prediction errors. A low RMSE indicates that the simulated values are close to the experimental data. In biomethanation modeling, an RMSE lower than 10% of the mean observed value is generally considered satisfactory [19]. R^2 represents the proportion of experimental variance explained by the model. A value of R^2 close to 1 indicates that the model can accurately reproduce the observed process dynamics, such as the cumulative methane yield or substrate degradation kinetics [18]. MAE is the mean of the absolute differences between the simulated and experimental values. It provides a direct measure of the average error and is less sensitive to outliers than RMSE. A small MAE indicates high overall predictive accuracy. The Pearson correlation coefficient (r) assesses the strength and direction of the linear relationship between simulated and experimental data. Values of r close to 1 confirm a strong positive correlation, meaning that the model correctly follows the trend of the experimental process [42].

In the context of anaerobic digestion, high values of R^2 (≥ 0.9) and r (≈ 1), combined with low RMSE and MAE, demonstrate good predictive performance of the model. These results confirm that the model can be used reliably to simulate methane production kinetics or organic matter degradation under various operating conditions [18,41].

The calculation code

We present in **Figure 3** the synoptic of the calculation code associated with two-phase modeling.

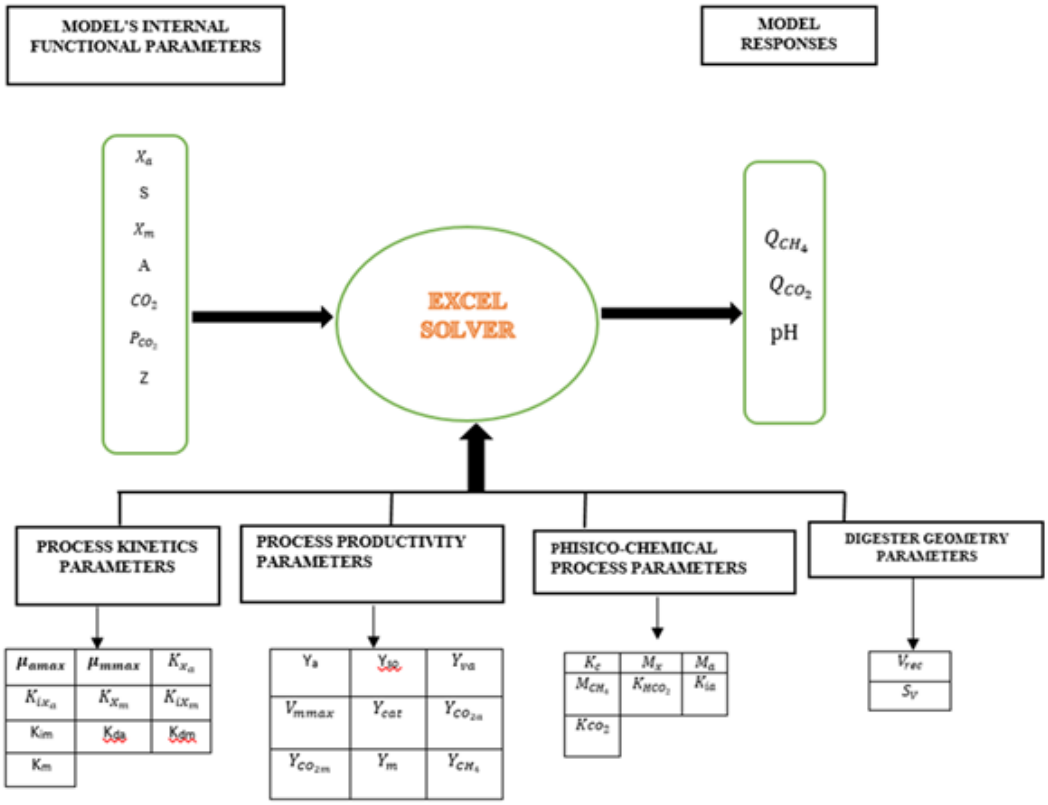

Figure 3. Synoptic diagram of the calculation code used for two-phase flow modeling

Computational and Experimental Research in Materials and Renewable Energy (CERiMRE)
Volume 8, Issue 2, page 175-206
eISSN : 2747-173X

Submitted : September 11, 2025
Accepted : November 12, 2025
Online : November 28, 2025
DOI : 10.19184/cerimre.v8i2.4

Experimentation

Inoculum preparation

The rumen juice used for inoculation was collected from the Masina abattoir, with two conditioning treatments applied: fresh (non-pretreated) and non-fresh (stored for 40 days in a sealed bottle)Fresh rumen juice: which has not undergone any pre-treatments.

Substrate preparation (corn straw)

The maize straw used in this study was harvested at the Masina walk of liberty, weighed with a SALTER brand balance and sun-dried for 10 days. It was then ground using a local-type grinder. Sun-drying facilitates the disintegration of the lignocellulosic material (straw). In fact, disintegration refers to the destruction of the cell membrane, allowing all intracellular material to be rejected. This process increases the amount of substrate available to micro-organisms and accelerates the rate of decomposition.

Shredding increases the total surface area of substrate available for biodegradation and thus for methanization. Generally speaking, although reducing particle size accelerates the rate of biodegradation, it does not necessarily increase gas yield [43]. Dry matter is determined by drying in an oven maintained at 105 ºC until the weight becomes constant. The difference in weight corresponds to the loss of moisture, and the residue represents the dry matter content of the sample.

Description of experimental set-up

The tests were carried out in batch reactors. These reactors are laboratory models, in polyethylene terephthalate (PET) plastic bottles (Figure 4), with a capacity of 1L, to ensure anaerobiosis of the medium. These reactors are fitted with two outlets, the first for taking liquid samples using a syringe, and the second for exhausting the gas into the gasometers via piping (perfusion kit) to measure the volume of biogas produced. These gasometers contain a 10% concentrated caustic soda solution (NaOH) for CO_2 absorption. The useful volume of the reactors is 800mL. We left a free volume above the liquid level to protect the gas outlet and ensure proper mixing.

We fed four reactors (**Figure 4**) as follows:

1) Digester I: fed at a loading rate of 7% DM and with a non-fresh inoculum.

2) Digester II: fed at a loading rate of 14% DM and containing non-fresh inoculum.

3) Digester III: with a feed rate of 7% DM and fresh inoculum.

4) Digester IV: fed at a loading rate of 14% DM and containing fresh inoculum.

Computational and Experimental Research in Materials and Renewable Energy (CERiMRE)
Volume 8, Issue 2, page 175-206
eISSN : 2747-173X

Submitted : September 11, 2025
Accepted : November 12, 2025
Online : November 28, 2025
DOI : 10.19184/cerimre.v8i2.4

Figure 4. Digesters

All four reactors were operated at room temperature and manually stirred once or twice a day. However, they were loaded at two different loading rates, 7% and 14%, and with different inoculum (rumen juice) conditioning. The inoculum represented 10% of the reactor volume. Dilutions were obtained by adding distilled water. Biogas volume measurement corresponds to the volume of liquid displaced in the gasometers.

Results and Discussion

Simulation results and discussion

pH evolution during anaerobic digestion

Two successive phases can be observed in **Figure 5**, the first is characterized by a rise in pH and the second by its stabilization at around 7~7.1.

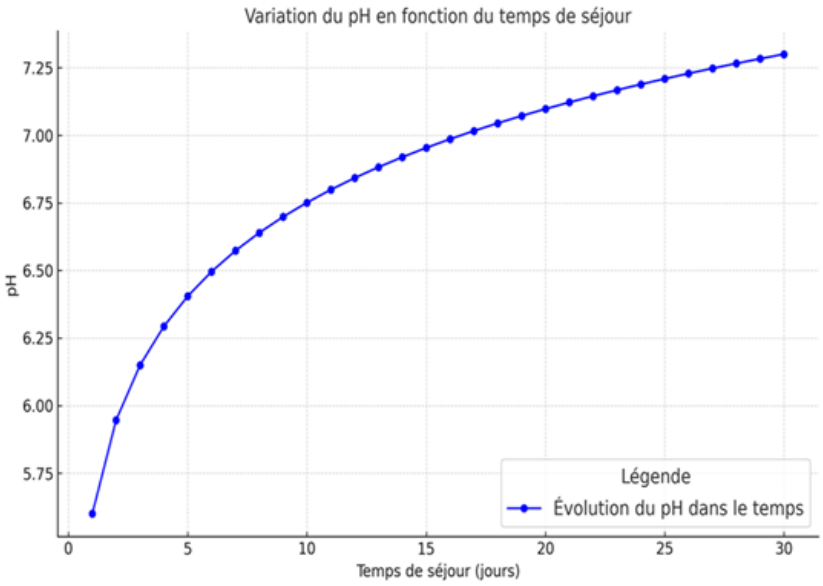

Figure 5. pH evolution during anaerobic digestion

Computational and Experimental Research in Materials and Renewable Energy (CERiMRE)
Volume 8, Issue 2, page 175-206
eISSN : 2747-173X

Submitted : September 11, 2025
Accepted : November 12, 2025
Online : November 28, 2025
DOI : 10.19184/cerimre.v8i2.4

Evolution of micro-organism growth

In the biological sense, growth is the ordered quantitative variation of all the constituents of an organism. In unicellular organisms, as in bacteria, growth results in an increase in the number of individuals and thus in the overall biomass. It should be noted that the initial presence of dissolved glucose in this model is 5 $g.l^{-1}$. The growth of the acid-generating biomass, which was on the increase, gradually diminishes to make way for the methanogenic population **Figure 6**. Growth of the methanogenic biomass is delayed, despite an increasing specific growth rate **Figure 7**.

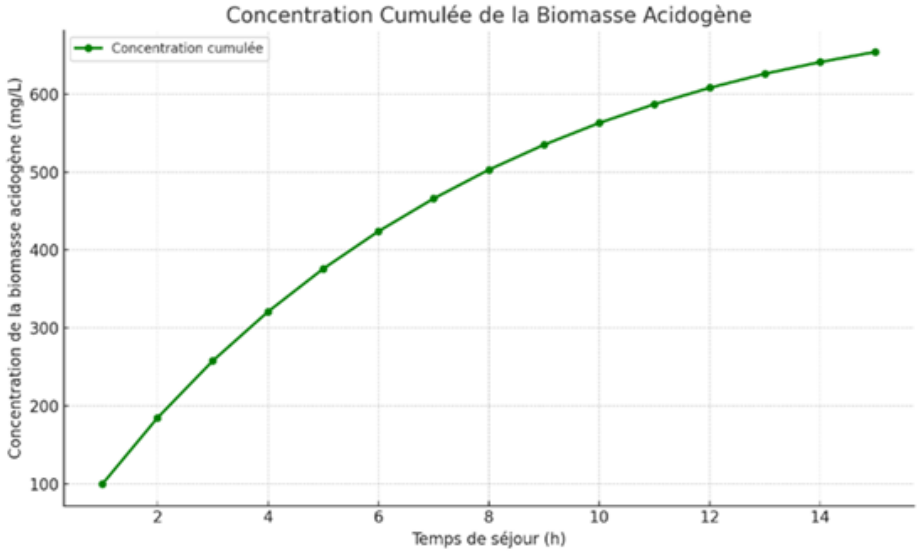

Figure 6. Evolution of acidogenesis biomass as a function of time

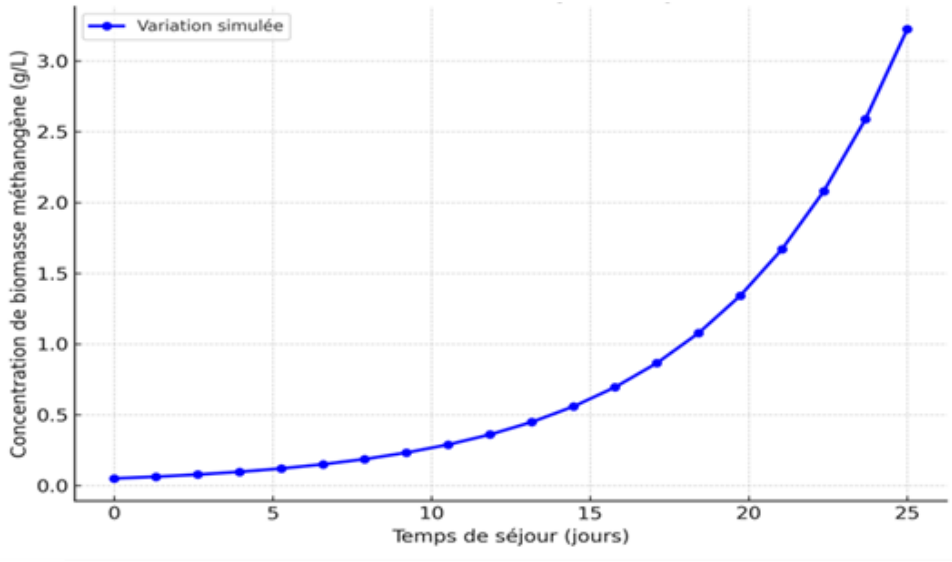

Figure 7. Evolution of methanogenic biomass as a function of time

Computational and Experimental Research in Materials and Renewable Energy (CERiMRE)
Volume 8, Issue 2, page 175-206
eISSN : 2747-173X

Submitted : September 11, 2025
Accepted : November 12, 2025
Online : November 28, 2025
DOI : 10.19184/cerimre.v8i2.4

Evolution of carbon dioxide flow rate

The evolution of carbon dioxide flow is shown in **Figure 8**.

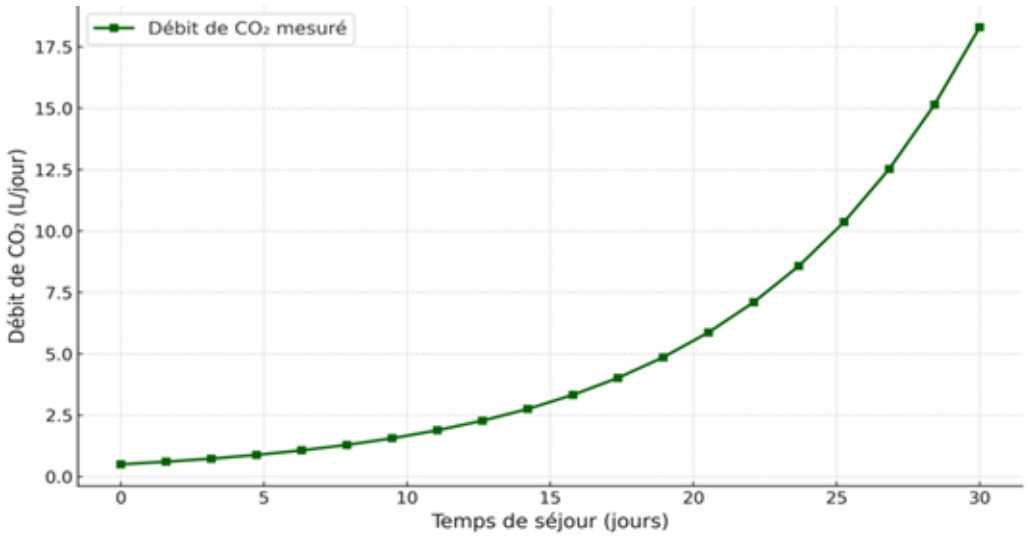

Figure 8. Evolution of CO_2 flow during contact time

Evolution of methane flow rate

The evolution of methane flow is shown in Figure 9.

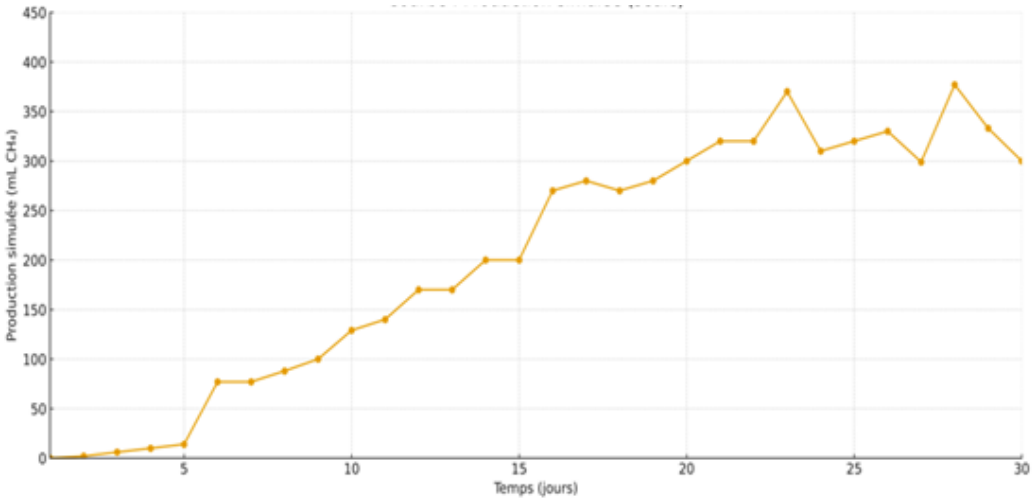

Figure 9. Evolution of flow rate of CH_4 as a function of time

We can see that biogas production increases around day 10, at a pH level favorable to bacterial growth and activity, i.e. between 6.6 and 7.1 (see **Figure 5** and **Figure 9**). During this phase, methane flow increases at a considerable rate due to the proliferation of methanogenic bacteria.

Computational and Experimental Research in Materials and Renewable Energy (CERiMRE)
Volume 8, Issue 2, page 175-206
eISSN : 2747-173X

Submitted : September 11, 2025
Accepted : November 12, 2025
Online : November 28, 2025
DOI : 10.19184/cerimre.v8i2.4

Simulation of biogas productivity has shown that the flow rate is irregular for both methane and carbon dioxide. The flow rate during the residence time is constantly increasing, but not at a constant rate. Flow levels appear over time, as an indirect consequence of limiting factors that may appear throughout the process.

Experimental results

Physico-chemical parameters of maize straw

Table 2 shows the average physico-chemical parameters of maize straw obtained from laboratory analyses. The (51.3%) moisture content obtained means that hydrolysis, the first stage in bio-methanization, can proceed normally. If, on the other hand, the moisture content is insufficient (below 50%), acidification takes place too quickly, to the detriment of bio-methanization. The dry matter content (48.7%) is very similar to the results of studies carried out by [44]. The organic matter value is significant because it means that in our straw sample, there is 78.4% material that can be degraded by micro-organisms.

Table 2. Average physico-chemical parameters of corn straw

TS (%)	OM (%)	TOC (%)	TON (%)	Ratio C/N
48.7	78.4	45.44	1.58	28.75

Methanogenic activity

The specific methanogenic activity was evaluated on the basis of the cumulative methane gas production curves). The correlation coefficients and the slope of the part with the highest production are shown in **Table 3**. The specific methanogenic activity expressed in mL-CH_4/g of organic matter (OM) inoculum per day is calculated according to the following expression:

$$Ac\ (in\ mL - CH_4/g\ of\ OM\ of\ inoculum\ day = \frac{slope}{dry\ matter\ rate\ per\ liter} \quad (33)$$

It should be noted that for all digesters, the rate of dry matter (DM) per liter of inocula was set at 100g DM/L. The results are shown in Table 3.

Table 3. Specific methanogenic activity expressed in mL CH_4 /g inoculum day organic matter

Digesters	Methanogenic activity
Digester 1	0.1516
Digester 2	0.1905
Digester 3	0.0658
Digester 4	0.0831

The comparative evaluation of methanogenic activity (**Table 3**) among the four digesters reveals distinct differences in microbial performance and substrate conversion efficiency. The measured values ranged from 0.0658 to 0.1905 mL CH_4 $g^{-1}{\cdot}j^{-1}$, reflecting variable methanogenic potentials under the applied operating conditions. Digester 2 (0.1905 mL CH_4 $g^{-1}{\cdot}j^{-1}$) recorded the highest methanogenic activity, indicating superior microbial efficiency in converting organic substrates into methane. This suggests optimal conditions for methanogenic archaea, likely supported by

Computational and Experimental Research in Materials and Renewable Energy (CERiMRE)
Volume 8, Issue 2, page 175-206
eISSN : 2747-173X

Submitted : September 11, 2025
Accepted : November 12, 2025
Online : November 28, 2025
DOI : 10.19184/cerimre.v8i2.4

stable pH, adequate nutrient availability, and a well-adapted inoculum. Such elevated activity values are typically associated with substrates rich in easily degradable compounds and favorable kinetic parameters [17], [18]. Digester 1 (0.1516 mL CH_4 $g^{-1}{\cdot}j^{-1}$) also demonstrated strong methanogenic performance, consistent with a well-balanced anaerobic process. The results suggest efficient coordination between hydrolytic–acidogenic and methanogenic phases, ensuring a steady conversion rate and minimal accumulation of intermediates.

Conversely, Digester 3 (0.0658 mL CH_4 $g^{-1}{\cdot}j^{-1}$) and Digester 4 (0.0831 mL CH_4 $g^{-1}{\cdot}j^{-1}$) exhibited substantially lower activities, implying suboptimal microbial functioning. These reduced rates may result from inhibitory factors (e.g., accumulation of volatile fatty acids or ammonia, nutrient deficiency) or the predominance of slowly degradable lignocellulosic materials that limit the availability of readily biodegradable carbon sources [18], [39]. The overall methanogenic activity followed the decreasing order: D2 > D1 >> D4 > D3, which aligns with the observed experimental methane production trends (**Figure 10 and Figure 11**).

The analysis of the methane production kinetics through the high production period, correlation coefficient, and slope values (**Table 4**) provides insight into the dynamics and efficiency of the anaerobic digestion process for each reactor.

Digester 1 exhibited a high production phase extending from day 4 to day 24, with a very high correlation coefficient (r = 0.9987) and a slope of 15.7, indicating an excellent linear relationship and a rapid methane generation rate during this period. This strong correlation reflects a highly stable and predictable biogas production phase, suggesting that the microbial community operated under near-optimal conditions. The relatively steep slope confirms a high substrate conversion rate and efficient methanogenic activity.

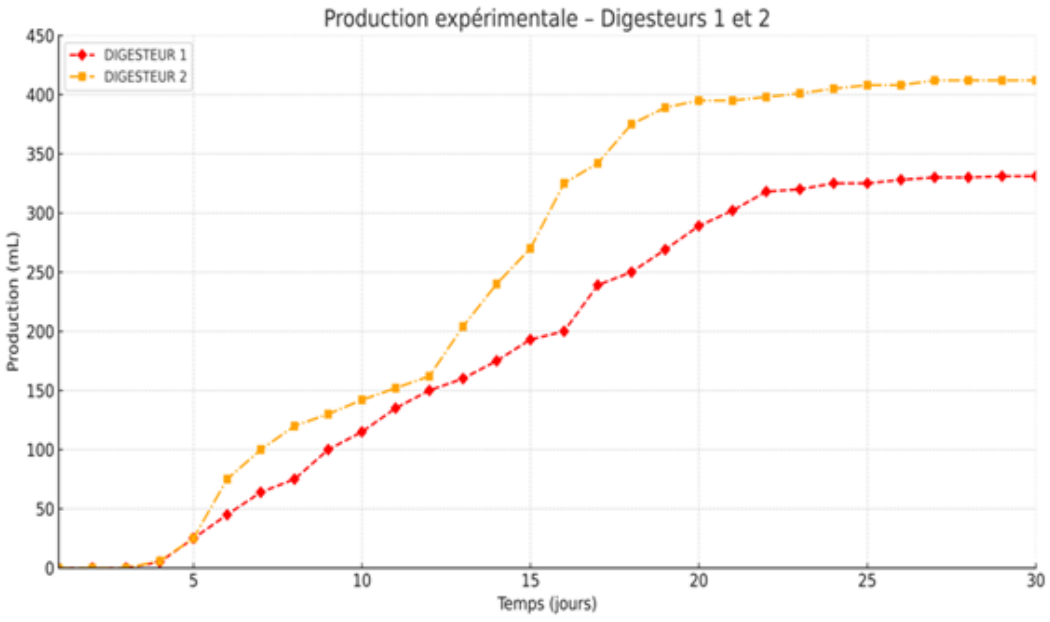

Figure 10. Cumulative methane gas production for digesters 1 and 2

Computational and Experimental Research in Materials and Renewable Energy (CERiMRE)
Volume 8, Issue 2, page 175-206
eISSN : 2747-173X

Submitted : September 11, 2025
Accepted : November 12, 2025
Online : November 28, 2025
DOI : 10.19184/cerimre.v8i2.4

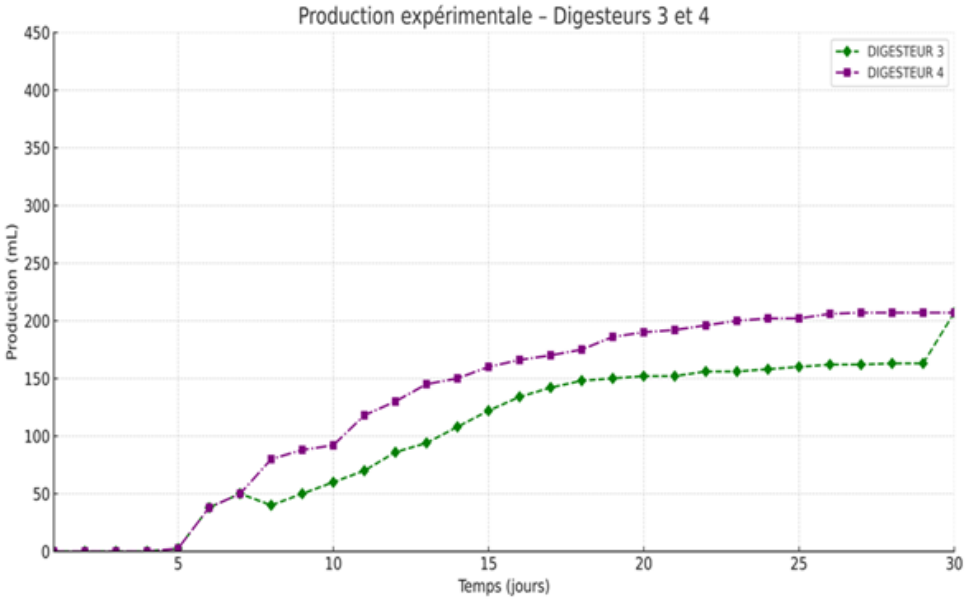

Figure 11. Cumulative methane gas production for digesters 3 and 4

Table 4. Correlation coefficients and slopes over the interval of highest production

Digesters	High production period in days	Correlation coefficients	Slope
Digester 1	4 – 24	0.9987	15.7
Digester 2	4 – 24	0.9465	19.052
Digester 3	6 – 25	0.9603	6.589
Digester 4	5 – 25	0.8654	8.71

Digester 2 also showed a high production period between days 4 and 24, with a correlation coefficient of 0.9465 and a slope of 19.052. Although the linear relationship is slightly weaker than that of D1, the higher slope indicates a more intense methane production rate. This could result from a higher concentration of easily degradable organic matter or faster microbial kinetics, even if accompanied by slightly greater fluctuations in gas production consistency.

In contrast, Digester 3 displayed a longer high production period (days 6 to 25) with a correlation coefficient of 0.9603 and a slope of 6.589. The correlation remains strong, but the lower slope suggests slower methane accumulation. This trend implies that the digestion process was more progressive, possibly due to the presence of moderately resistant organic fractions or slower microbial adaptation.

Digester 4 exhibited the lowest correlation coefficient (r = 0.8654) and a slope of 8.71, with a production period from day 5 to day 25. The reduced linearity indicates greater variability in gas production, likely caused by metabolic inhibition or inconsistent degradation of complex substrates. The moderate slope suggests a lower methane productivity rate, reflecting less efficient methanogenic activity.

In fact, digesters 1 and 2, which were fed with non-fresh inoculum, exhibited a higher methanogenic capacity compared to digesters 3 and 4 (**Table 3**). This inoculum, derived from

Computational and Experimental Research in Materials and Renewable Energy (CERiMRE)
Volume 8, Issue 2, page 175-206
eISSN : 2747-173X

Submitted : September 11, 2025
Accepted : November 12, 2025
Online : November 28, 2025
DOI : 10.19184/cerimre.v8i2.4

rumen juice preserved for 40 days, promotes effective proliferation of methanogenic bacteria specifically adapted to the corn straw substrate. The methanogenic activity test reflects the functional response of these bacteria in the presence of the target substrate. It is therefore crucial to inoculate the fermenter with a microbial consortium that demonstrates optimal activity with the selected substrate. Using a stabilized inoculum with high specific methanogenic activity can help mitigate the primary challenge in anaerobic digestion: the imbalance between acidogenesis, a rapid step, and methanogenesis, which proceeds more slowly. Our experiments clearly demonstrate that the nature of the inoculum plays a pivotal role in shaping microbial community dynamics, as it balances populations with widely differing growth rates.

The highest cumulative methane yields were observed in digesters 1 and 2, reaching 330 mL and 412 mL, respectively, in an 800 mL reactor over 28 days (**Figure 10**). In contrast, digesters 3 and 4 produced substantially less methane, with cumulative values of 153 mL and 197 mL, respectively (**Figure 11**). Simulation results indicate that methane production is maximized within a pH range of 6.6 to 7.2, which provides favorable conditions for the microbial populations present in the medium (**Figure 5**). Within this range, methane flow significantly increases (**Figure 7**), likely due to rapid proliferation of methanogenic biomass, thereby accelerating methanogenesis (**Figure 9**).

Theoretical simulations further reveal that methane production in digesters 1 and 2 initiates as soon as the lower threshold of the optimal pH is reached (day 4). Conversely, digesters 3 and 4, despite having similar pH conditions, show delayed start-up phases on days 5 and 6, respectively (**Figure 9**). This lag can be attributed to the adaptation period required by bacterial populations in these digesters. Notably, the non-fresh rumen juice achieved the highest methane yields, as its pre-conditioning facilitated rapid bacterial activation, which in turn enhanced the degradation of lignocellulosic material. Across all four digesters, methane yield increased with the organic loading rate, suggesting that the optimal loading rate for these systems may be higher than those tested. This underscores the importance of tailoring inoculum characteristics and operating parameters to the specific substrate to maximize methanogenic efficiency.

Validation

The validation results are presented in **Figure 12**, **Figure 13**, **Figure 14**, and **Table 5**. The comparison between simulated and experimental pH values shows a good overall consistency between the model and the measurements obtained from the four digesters (**Figure 12**). The pH gradually increases from an acidic phase (around 5.8) to a neutral or slightly basic range (approximately 7.2–7.4), indicating a progressive stabilization of the anaerobic digestion process. Digesters 1, 2, and 3 exhibit a strong correlation with the simulated pH, with minor variations and a well-reproduced trend, reflecting stable microbiological kinetics and a well-calibrated simulation model. Digester 4, which shows greater fluctuations, presents some occasional deviations not captured by the model, likely due to local experimental disturbances. Statistically, the results (r = 0.835; R^2 = 0.604; MAE = 0.307; RMSE = 0.364) confirm a strong correlation and satisfactory accuracy between simulated and experimental pH values. Overall, the model accurately reproduces the real pH dynamics over time and can be considered reliable for predicting the global behavior of the system.

Computational and Experimental Research in Materials and Renewable Energy (CERiMRE)
Volume 8, Issue 2, page 175-206
eISSN : 2747-173X

Submitted : September 11, 2025
Accepted : November 12, 2025
Online : November 28, 2025
DOI : 10.19184/cerimre.v8i2.4

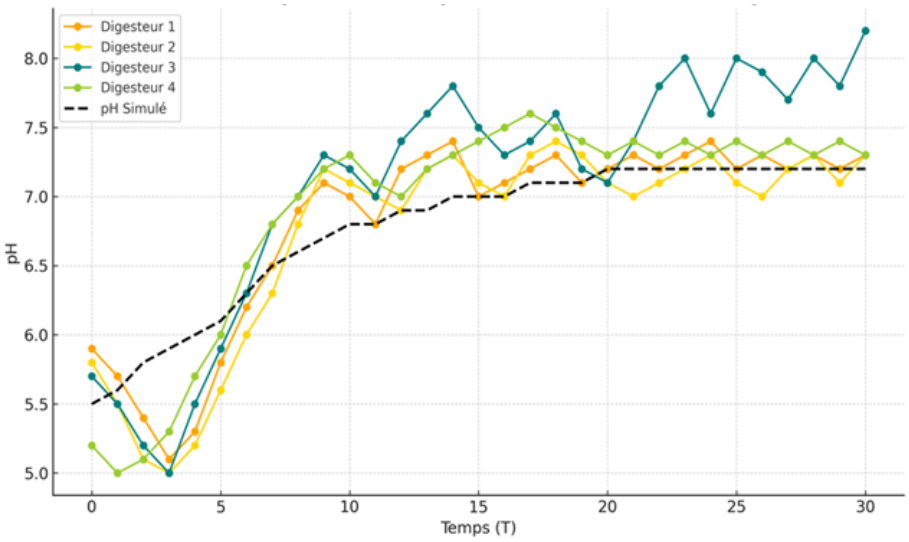

Figure 12. Comparative graph of simulated and experimental pH

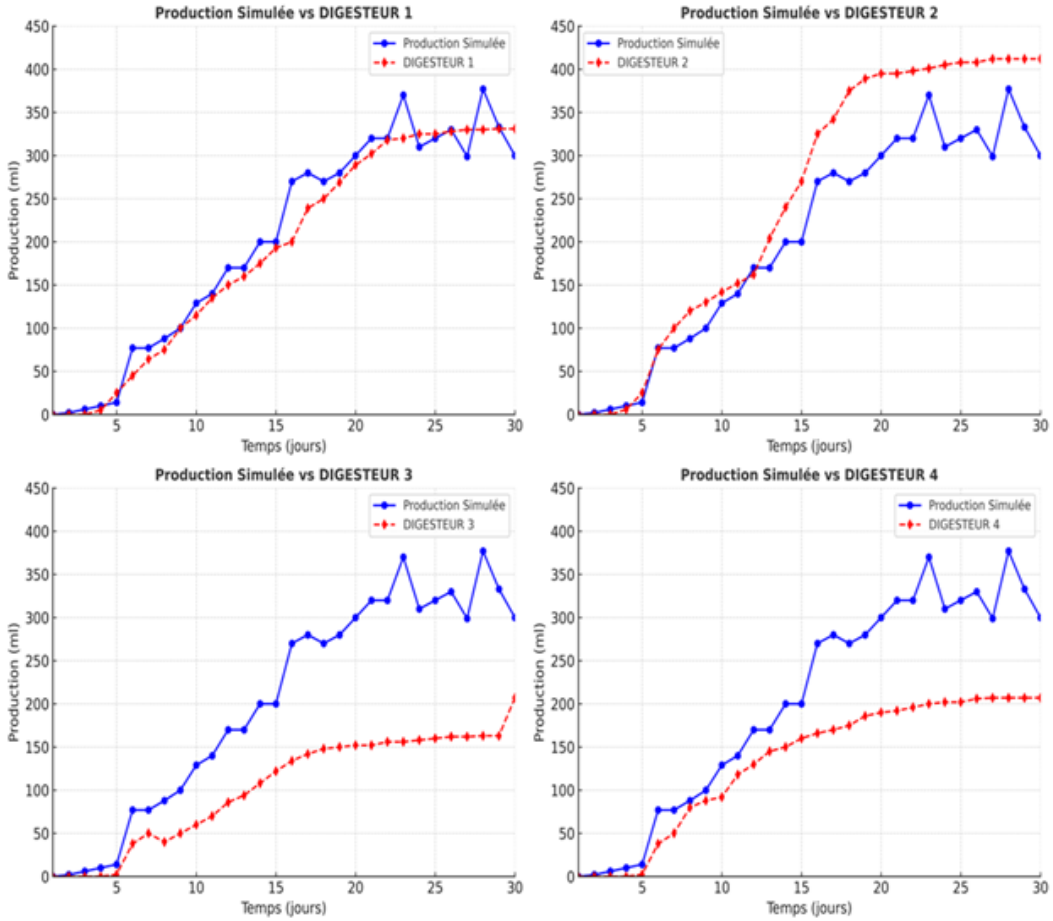

Figure 13. Comparison of simulated and experimental production for each digester

Computational and Experimental Research in Materials and Renewable Energy (CERiMRE)
Volume 8, Issue 2, page 175-206
eISSN : 2747-173X

Submitted : September 11, 2025
Accepted : November 12, 2025
Online : November 28, 2025
DOI : 10.19184/cerimre.v8i2.4

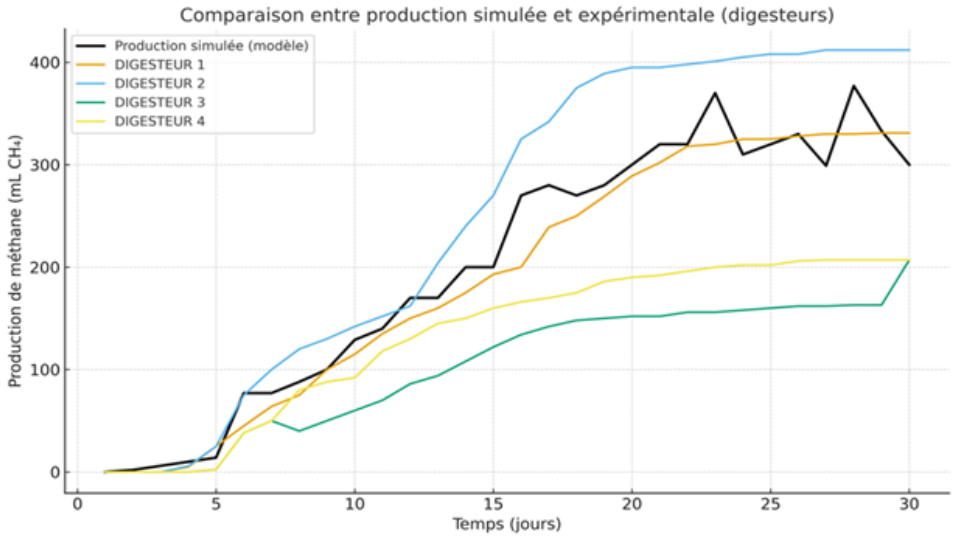

Figure 14. Comparison of simulated and experimental production for all four digesters

Table 5. Statistical Evaluation of the Biphasic Model for the Four Digesters

Digesters	Correlation coefficient (r)	Coefficient of Determination (R^2)	RMSE (mL CH_4)	MAE (mL CH_4)	Interpretation
D1	0.975	0.951	22.4	15.8	Excellent correlation; the simulated curve almost perfectly matches Digester 1, especially in the growth and stabilization phases.
D2	0.958	0.918	33.6	23.5	Very good correlation; small deviation during the peak production phase.
D3	0.902	0.814	39.2	27.0	Moderate co-production and shows variability relation; the model underestimates early mid-phase.
D4	0.860	0.740	35.5	25.2	Fair correlation; the model slightly overpredicts final methane production levels.

Statistical evaluation of the agreement between simulated and experimental methane productions was performed for the four digesters (D1, D2, D3, and D4) using correlation coefficient (r), coefficient of determination (R^2), root mean square error (RMSE), and mean absolute error (MAE). The results confirm a generally strong performance of the applied biphasic model, indicating that it successfully reproduces the main kinetic trends of methane production under batch conditions (**Figure 12** and **Figure 13**).

For Digester 1, both the correlation ($r \approx 0.98$) and determination ($R^2 \approx 0.95$) coefficients highlight an excellent agreement between simulated and measured values (**Table 5**). The statistical errors

Computational and Experimental Research in Materials and Renewable Energy (CERiMRE)
Volume 8, Issue 2, page 175-206
eISSN : 2747-173X

Submitted : September 11, 2025
Accepted : November 12, 2025
Online : November 28, 2025
DOI : 10.19184/cerimre.v8i2.4

remain low (RMSE ≈ 22 mL, MAE ≈ 16 mL), reflecting the model's high predictive accuracy. The simulation effectively captures all three kinetic phases — the initial lag phase (days 1–3), the exponential increase (days 5–15), and the stabilization period from day 25 onwards — demonstrating robust parameterization of the hydrolysis and methanogenesis rates.

For Digester 2, the correlation (r ≈ 0.96, R^2 ≈ 0.92) also denotes a very good fit, although slightly below that of D1. The deviations observed (RMSE ≈ 34 mL, MAE ≈ 23 mL) are primarily associated with the model's underestimation of the production peak (~410 mL). This discrepancy likely results from faster substrate conversion in the experimental setup, which reached its plateau earlier than predicted. Such behavior suggests that the model's hydrolysis constant could be adjusted to account for more reactive or easily degradable organic fractions.

For Digester 3, the agreement remains moderate to good (r ≈ 0.90, R^2 ≈ 0.81), with RMSE and MAE values (≈ 39 and 27 mL, respectively) indicating noticeable but acceptable deviations. The model underestimates methane production during the mid-phase (days 10–20), possibly due to fluctuating microbial activity or uneven substrate accessibility, which would influence the degradation kinetics of intermediate compounds.

For Digester 4, the correlation is fair but weaker (r ≈ 0.86, R^2 ≈ 0.74). The model slightly overestimates methane production toward the final phase, as seen in Figures 12–13. This suggests that the applied kinetic constants may not fully represent the slower stabilization process observed experimentally. The deviations (RMSE ≈ 35 mL; MAE ≈ 25 mL) could result from microbial inhibition or a reduced methanogenic efficiency during the late digestion phase, possibly due to substrate depletion or accumulation of inhibitory intermediates.

Overall, the obtained results fall within the performance range reported for validated anaerobic digestion models: 1) $R^2 > 0.80$: indicative of a reliable fit [17], [18], and 2) RMSE < 10–20% of the maximum methane yield: model considered acceptable for kinetic simulations [40]. Hence, the applied biphasic model provides a realistic and quantitatively accurate representation of the digestion kinetics, particularly for D1 and D2. The lower predictive performance observed for D4 could be mitigated through targeted recalibration of kinetic parameters, such as slower hydrolysis rates or extended acidogenesis duration, to better capture the delayed stabilization and possible inhibitory effects.

The indicators obtained in this study (r = 0.86–0.98; R^2 = 0.74–0.95; RMSE = 22–39 mL CH_4; MAE = 16–27 mL CH_4) indicate that the biphasic model provides an accurate and reliable description of methane production kinetics across the four digesters. These values are fully consistent with, and in some cases superior to, those reported in previous modeling studies of batch anaerobic digestion.

[18] and [19] reported R^2 values typically ranging between 0.80 and 0.95 for ADM1-based models applied to various substrates, with RMSE generally below 15–25% of the maximum methane yield. The performance obtained here (R^2 up to 0.95 for D1 and D2, and RMSE ≤ 10% of the maximum production) thus falls within the upper range of reported accuracies. In a study by [40] on co-digestion of food waste and sludge, the biphasic first-order model achieved R^2 between 0.82 and 0.90, with RMSE values around 30–50 mL CH_4. The present results for D1 and D2 (R^2 = 0.95 and 0.92, RMSE = 22–34 mL CH_4) demonstrate higher predictive precision, likely due to better calibration of hydrolysis and methanogenesis parameters.

Computational and Experimental Research in Materials and Renewable Energy (CERiMRE)
Volume 8, Issue 2, page 175-206
eISSN : 2747-173X

Submitted : September 11, 2025
Accepted : November 12, 2025
Online : November 28, 2025
DOI : 10.19184/cerimre.v8i2.4

Similarly, modeled lignocellulosic biomass digestion using a modified Gompertz equation [37] and reported RMSE [45] values around 35–45 mL CH_4 and MAE ≈ 25–30 mL CH_4, close to those found for D3 and D4 in this work. The comparable level of error suggests that the deviations observed here are within the expected range for heterogeneous substrates where hydrolysis is the rate-limiting step.

The performance of the biphasic model developed in this study can be compared with that reported by [28], who investigated the modeling of methane production and biogas quality in a methanogenic digester. Hess applied a mechanistic approach to simulate the fermentation dynamics and observed a satisfactory agreement between experimental and simulated data, with reported coefficients of determination generally ranging between 0.80 and 0.90, depending on substrate composition and operational conditions. In comparison, the present model achieved higher statistical performance, with correlation coefficients (r) between 0.86 and 0.98 and coefficients of determination (R^2) from 0.74 to 0.95, demonstrating a stronger predictive capacity for methane yield, particularly for Digesters 1 and 2. The relatively lower deviations (RMSE = 22–39 mL CH_4; MAE = 16–27 mL CH_4) also indicate an improvement in model calibration and sensitivity to kinetic parameters compared to the results of [28], whose simulations were more influenced by system variability and substrate heterogeneity. Overall, these findings suggest that the biphasic model developed here provides equal or superior predictive accuracy relative to the earlier work of [28], while maintaining strong consistency with the experimental behavior of the digestion process

Overall, the present findings demonstrate that the biphasic model performs within or above the statistical standards reported in the literature for anaerobic digestion modeling. Its predictive accuracy for D1 and D2 confirms the model's ability to reproduce both the rapid hydrolytic stage and the slower methanogenic stage, while the moderate deviations for D3 and D4 highlight expected variability due to substrate complexity and microbial heterogeneity. The biphasic model applied in this study accurately reflects the behavior of the digesters, particularly for D1 and D2. The discrepancies observed for D4 suggest the presence of an inhibition effect or variability in the inoculum, which the model could account for through a specific calibration of the kinetic parameters (e.g., slower hydrolysis or prolonged acidogenesis).

Conclusions

The present study focused on the valorization of corn straw through biomethanization, combining experimental investigation and theoretical modeling to optimize methane production. A biphasic kinetic simulation was applied to monitor the evolution of key physicochemical parameters and evaluate the performance of laboratory-scale digesters. To promote efficient degradation of lignocellulosic biomass, the substrate was inoculated with rumen juice collected from the Masina slaughterhouse, while two inoculum conditioning methods were tested to assess enzymatic activity and methanogenic potential. Experimental results from the four batch digesters revealed that biogas productivity strongly depends on substrate composition, microbial activity, mixing efficiency, temperature regulation, loading rate, and pH stability. Among the systems, Digesters D1 and D2 achieved the highest methane yields, with D2 showing the best overall performance due to its higher organic loading rate and improved substrate–microbe contact.

The biphasic kinetic model provided an accurate representation of methane production dynamics. Statistical validation showed excellent predictive performance for D1 (R^2 = 0.951, r = 0.975) and

Computational and Experimental Research in Materials and Renewable Energy (CERiMRE)
Volume 8, Issue 2, page 175-206
eISSN : 2747-173X

Submitted : September 11, 2025
Accepted : November 12, 2025
Online : November 28, 2025
DOI : 10.19184/cerimre.v8i2.4

very good agreement for D2 (R^2= 0.918, r = 0.958), with low RMSE and MAE values, confirming the robustness of the simulation. Moderate correlations for D3 (R^2= 0.814) and fair agreement for D4 (R^2 = 0.740) indicate that additional calibration of the hydrolysis and methanogenesis parameters could further refine the model's predictive capacity. These trends are consistent with results reported in litteratures , where R^2 values between 0.75 and 0.95 are typically observed for calibrated anaerobic digestion models of lignocellulosic substrates. The model successfully captured the critical influence of pH (6.6–7.2) and hydraulic retention time (~30 days) on methane generation, confirming that maintaining these parameters within optimal ranges is essential for process stability and microbial efficiency.

Overall, the study demonstrates that the biphasic model is a reliable and powerful tool for simulating and optimizing methane production from corn straw. The strong agreement between simulation and experimental data for D1 and D2 validates the model's applicability to lignocellulosic substrates. Future work should focus on scaling up the process to pilot or industrial levels to evaluate technical feasibility and economic viability. Co-digestion with complementary organic wastes could improve nutrient balance and enhance methane yield, while metagenomic analysis of microbial communities would offer valuable insights into microbial interactions and process optimization. Finally, integrating this biomethanization process into a circular bioeconomy framework could significantly contribute to renewable energy generation, agricultural waste valorization, and greenhouse gas mitigation.

ACKNOWLEDGEMENTS
We sincerely thank the Faculty of Oil, Gas, and Renewable Energy for their support in facilitating this research.

List of Acronyms and Symbols

The following abbreviations are used in this manuscript:

A	:	total concentration of acetic acid (g.L^{-1})
A_h	:	concentration of non-ionized acetic acid (g.L^{-1})
A_{inf}	:	acetic acid concentration of the influent (g.L^{-1})
CH_4	:	production of methane (g.L^{-1})
$[CO_2]$	:	concentration of CO_2 dissolved in the effluent (mol.L^{-1})
D	:	dilution rate (j^{-1})
H^+	:	hydrogen ion concentration (mol.L^{-1})
HCO_3^-	:	bicarbonate concentration of the effluent (mol.L^{-1})
k_c	:	acid dissociation constant
k_{CO_2}	:	CO_2 ionization constant
k_{da}	:	rate of decrease of acidogenic biomass (j^{-1})
k_{dm}	:	rate of decay of methanogenic biomass (j^{-1})
k_{HCO_2}	:	Henry's constant for CO_2 (mol/mmHg/l)
k_{im}	:	acetic acid inhibition constant on methane production (g.L^{-1})
k_{ix_m}	:	constant for inhibiting the growth of acidogenic bacteria (g.L^{-1})
k_{ia}	:	gas transfer coefficient (g.L^{-1})
k_m	:	saturation constant of methane production (g.L^{-1})
k_{x_a}	:	saturation constant for the growth of acidogenic bacteria (g.L^{-1})
k_{x_m}	:	saturation constant of the growth of methanogenic bacteria (g.L^{-1})
M_a	:	molar mass of acetic acid (g.mol^{-1})

Computational and Experimental Research in Materials and Renewable Energy (CERiMRE)
Volume 8, Issue 2, page 175-206
eISSN : 2747-173X

Submitted : September 11, 2025
Accepted : November 12, 2025
Online : November 28, 2025
DOI : 10.19184/cerimre.v8i2.4

M_{CH_4}	:	molar mass of methane (g.mol^{-1})
M_x	:	molar mass of the organism (g.mol^{-1})
P_{CO_2}	:	partial pressure of CO_2 in gas phase (mmHg)
Q	:	total flow (L.j^{-1})
Q_{CO_2}	:	CO_2 flow rate (L.j^{-1})
Q_{CH_4}	:	flow rate of CH_4 (L.j^{-1})
RAC	:	rate of formation of CO_2 linked to the production of acetic acid (mol.L^{-1}.j^{-1})
R_{AF}	:	rate of formation of CO_2 by the action of acidogenic biomasses (mol.L^{-1}.j^{-1})
R_Z	:	rate of CO_2 consumption due to the release of the (mol.L^{-1}.j^{-1})
RM	:	rate of CO_2 production by the action of methanogenic biomasses (mol.L^{-1}.j^{-1})
S	:	glucose equivalent concentration of the substrate (g.L^{-1})
S_V	:	standard volume (L.mol^{-1})
V_{mmax}	:	maximum rate of methane production (in g) per gram of methanogenic bacteria per day (g.g^{-1}.j^{-1})
V_{rec}	:	reactor volume (L)
μ_a	:	specific rate (speed) of growth of the acidogenic bacterial community (j^{-1})
μ_{amax}	:	maximum rate (speed) of specific growth of acidogenic biomass (j^{-1})
μ_m	:	specific rate of growth of methanogenic biomass (j^{-1})
μ_{mmax}	:	maximum rate (speed) of specific growth of methanogenic biomass (j^{-1})
X	:	concentration of substrate or biomass according to indices (g.L^{-1})
Y_a	:	yield coefficient linked to the degradation of the complex substrate caused by acidogenic bacteria (g.g^{-1})
Y_{cat}	:	the yield coefficient of the formation of this cation due to the action of acidogenic bacteria (g.g^{-1})
Y_{so}	:	yield coefficient linked to the formation of soluble organic matter (g.g^{-1})
Y_{va}	:	yield coefficient of the conversion of the substrate into acetic acid by the acidogenic biomass (g.g^{-1})
Y_m		yield coefficient linked to the consumption of acetic acid by methanogenic biomass (g.g^{-1})
$Y_{CO_{2m}}$		coefficient of CO2 production efficiency by methanogenic biomasses (g.g^{-1})
Z		concentration of cations (g.L^{-1})
Z_{inf}		concentration of cations in the influent (g.L^{-1})

References

[1] P. Dalal, “Challenges of Global Warming in 21th Centaury,” vol. 15, no. 2, pp. 95–105, 2025.

[2] Z. Lyu, N. Shao, T. Akinyemi, and W. B. Whitman, “Methanogenesis,” *Curr. Biol.*, vol. 28, no. 13, pp. R727–R732, 2018.

[3] I. Mvovo, “Impact of Climate Change on Biodiversity,” *Prog. Phys. Geogr.*, vol. 39, pp. 460–482, 2021.

[4] D. Viaggi, *Exploring the Economics of the Circular Bioeconomy*. 2020. doi: 10.1007/978-981-15-7321-7_1.

[5] E. P. Wulandari, E. Yulihastin, S. Zehri, and B. F. Nugraha, “Agroclimatic Suitability of Biomass Sorghum in West Java, Indonesia: A CLIMEX-Based Study for Renewable Energy Development,” *Comput. Exp. Res. Mater. Renew. Energy*, vol. 8, no. 1, pp. 30–43, 2025.

Computational and Experimental Research in Materials and Renewable Energy (CERiMRE)
Volume 8, Issue 2, page 175-206
eISSN : 2747-173X

Submitted : September 11, 2025
Accepted : November 12, 2025
Online : November 28, 2025
DOI : 10.19184/cerimre.v8i2.4

[6] G. Herrera-Franco, E. Alarcón-Rodríguez, L. Bravo-Montero, J. Caicedo-Potosí, and E. Berrezueta, “Analysis of decentralized energy systems in rural communities: A focus on accessibility and sustainability,” *Chall. Sustain*, vol. 13, no. 4, pp. 477–492, 2025.

[7] C. E. Manyi-Loh and R. Lues, “Anaerobic digestion of lignocellulosic biomass: substrate characteristics (challenge) and innovation,” *Fermentation*, vol. 9, no. 8, p. 755, 2023.

[8] J. Wang, S. Liu, K. Feng, Y. Lou, J. Ma, and D. Xing, “Anaerobic digestion of lignocellulosic biomass: Process intensification and artificial intelligence,” *Renew. Sustain. Energy Rev.*, vol. 210, p. 115264, 2025.

[9] M. Hassan, M. Umar, W. Ding, E. Mehryar, and C. Zhao, “Methane enhancement through co-digestion of chicken manure and oxidative cleaved wheat straw: Stability performance and kinetic modeling perspectives,” *Energy*, vol. 141, pp. 2314–2320, 2017.

[10] B. J. Poddar *et al.*, “A comprehensive review on the pretreatment of lignocellulosic wastes for improved biogas production by anaerobic digestion,” *Int. J. Environ. Sci. Technol.*, vol. 19, no. 4, pp. 3429–3456, 2022.

[11] M. Ramin, D. Lerose, F. Tagliapietra, and P. Huhtanen, “Comparison of rumen fluid inoculum vs. faecal inoculum on predicted methane production using a fully automated in vitro gas production system,” *Livest. Sci.*, vol. 181, pp. 65–71, 2015, doi: 10.1016/j.livsci.2015.09.025.

[12] Q. Yu, C. Sun, W. Cao, R. Liu, M. H. Abd-Alla, and A.-H. M. Rasmey, “Rumen fluid pretreatment promotes anaerobic methane production: revealing microbial dynamics driving increased acid yield from different concentrations of corn straw,” *Environ. Sci. Pollut. Res.*, pp. 1–15, 2024.

[13] B. Žalys, K. Venslauskas, and K. Navickas, “Microbial pretreatment for biogas: analyzing dairy rumen anaerobic bacteria inoculum’s impact on alfalfa biomass and energy value,” *Processes*, vol. 11, no. 12, p. 3384, 2023.

[14] B. Žalys, K. Venslauskas, K. Navickas, E. Buivydas, and M. Rubežius, “The Influence of Dairy Rumen Anaerobic Bacteria Inoculum on Biogas Production,” *Eng. Proc.*, vol. 37, no. 1, p. 83, 2023.

[15] L. S. Paraschiv and S. Paraschiv, “Contribution of renewable energy (hydro, wind, solar and biomass) to decarbonization and transformation of the electricity generation sector for sustainable development,” *Energy Reports*, vol. 9, pp. 535–544, 2023.

[16] X. Lu, H. Wang, F. Ma, G. Zhao, and S. Wang, “Enhanced anaerobic digestion of cow manure and rice straw by the supplementation of an iron oxide–zeolite system,” *Energy & Fuels*, vol. 31, no. 1, pp. 599–606, 2017.

Computational and Experimental Research in Materials and Renewable Energy (CERiMRE)
Volume 8, Issue 2, page 175-206
eISSN : 2747-173X

Submitted : September 11, 2025
Accepted : November 12, 2025
Online : November 28, 2025
DOI : 10.19184/cerimre.v8i2.4

[17] T. Menzel, P. Neubauer, and S. Junne, “Role of microbial hydrolysis in anaerobic digestion,” *Energies*, vol. 13, no. 21, 2020, doi: 10.3390/en13215555.

[18] I. Angelidaki and M. Alves, “Anaerobic Biodegradation, Activity and Inhibition.” Lyngby, 2006.

[19] D. J. Batstone *et al.*, “The IWA anaerobic digestion model no 1 (ADM1),” *Water Sci. Technol.*, vol. 45, no. 10, pp. 65–73, 2002.

[20] B. Jankovičová, M. Hutňan, and M. Sammarah, “Enhancing Biogas Production: Pre-Treatment of Lignocellulosic Biomass Using Biogas Plant Digestate,” *Sustain.*, vol. 17, no. 9, 2025, doi: 10.3390/su17093898.

[21] D. Morau, “Modelling of the devices of energy revalorization of solid waste and liquids: drying, anaerobic fermentation, thermal oxidation: implemented of a tool of assistance at design multi-systems multi-models,” Universite de la Reunion, Faculte des Sciences de l’Homme et de l'Environnement, Laboratoire de Physique du Batiment et des Systemes (France), 2006.

[22] T. E. Lesenyeho, “Investigating viability of using solar.” National University of Lesotho, 2021.

[23] J. Wu, H. Zhang, Y. Zhao, X. Yuan, and Z. Cui, “Effect of Temperature on the Inocula Preservation, Mesophilic Anaerobic Digestion Start-Up, and Microbial Community Dynamics,” *Agronomy*, vol. 14, no. 12, 2024, doi: 10.3390/agronomy14122991.

[24] H. Qiang, D. L. Lang, and Y. Y. Li, “High-solid mesophilic methane fermentation of food waste with an emphasis on Iron, Cobalt, and Nickel requirements,” *Bioresour. Technol.*, vol. 103, no. 1, pp. 21–27, Jan. 2012, doi: 10.1016/j.biortech.2011.09.036.

[25] A. Martinez, L. Vernieres-Hassimi, L. Abdelouahed, B. Taouk, C. Mohabeer, and L. Estel, “Modelling of an Anaerobic Digester: Identification of the Main Parameters Influencing the Production of Methane Using the Sobol Method,” *Fuels*, vol. 3, no. 3, pp. 436–448, 2022, doi: 10.3390/fuels3030027.

[26] J. Monod, “The growth of bacterial cultures,” *Sel. Pap. Mol. Biol. by Jacques Monod*, vol. 139, p. 606, 2012.

[27] Z. Zahan, M. Z. Othman, and T. H. Muster, “Anaerobic digestion/co-digestion kinetic potentials of different agro-industrial wastes: A comparative batch study for C/N optimisation,” *Waste Manag.*, vol. 71, pp. 663–674, 2018.

[28] J. Hess, “Modélisation de la qualité du biogaz produit par un fermenteur méthanogène et stratégie de régulation en vue de sa valorisation.” Université Nice Sophia Antipolis, 2007.

Computational and Experimental Research in Materials and Renewable Energy (CERiMRE)
Volume 8, Issue 2, page 175-206
eISSN : 2747-173X

Submitted : September 11, 2025
Accepted : November 12, 2025
Online : November 28, 2025
DOI : 10.19184/cerimre.v8i2.4

[29] J. F. Andrews, “A mathematical model for the continuous culture of microorganisms utilizing inhibitory substrates,” *Biotechnol. Bioeng.*, vol. 10, no. 6, pp. 707–723, 1968.

[30] E. C. van der Pol, “Development of a lactic acid production process using lignocellulosic biomass as feedstock.” Wageningen University and Research, 2016.

[31] K. Nadeem *et al.*, “Modeling, simulation and control of biological and chemical P-removal processes for membrane bioreactors (MBRs) from lab to full-scale applications: State of the art,” *Sci. Total Environ.*, vol. 809, p. 151109, 2022.

[32] Y. Vögeli, C. Riu, A. Gallardo, S. Diener, and C. Zurbrügg, *Anaerobic Digestion of Biowaste in Developing Countries*. 2014.

[33] M. U. Yunus, K. Silas, A. L. Yaumi, and B. H. Kwaji, “Kinetic Study of Microbial Growth in Anaerobic Digestion of Solid Waste,” *Int. J. Sci. Multidiscip. Res*, vol. 1, pp. 1119–1130, 2023.

[34] M. Tcha-Thom, “Recherche d’une filière durable pour la méthanisation des déchets de fruits et d’abattoirs du Togo: Evaluation du potentiel agronomique des digestats sur les sols de la région de la Kara.” Université de Limoges; Université de Lomé (Togo), 2019.

[35] I. Ostos, L. M. Flórez-Pardo, and C. Camargo, “A metagenomic approach to demystify the anaerobic digestion black box and achieve higher biogas yield: a review,” *Front. Microbiol.*, vol. 15, p. 1437098, 2024.

[36] S. Wang, N. C. Rao, R. Qiu, and R. Moletta, “Performance and kinetic evaluation of anaerobic moving bed biofilm reactor for treating milk permeate from dairy industry,” *Bioresour. Technol.*, vol. 100, no. 23, pp. 5641–5647, 2009.

[37] L. Lower, Y. Qiu, R. C. Sartor, W. J. Sagues, and J. J. Cheng, “Kinetic Modeling of Thermophilic Anaerobic Digestion of Lemnaceae for Biogas Production,” *BioEnergy Res.*, vol. 18, no. 1, p. 23, 2025.

[38] D. Wu *et al.*, “Multidimensional insights into efficiency-stability trade-off in anaerobic digestion from organic overloading stress: Kinetic behavior, energy harvesting, and genome-centric metagenomics microbial self-adaptation,” *Water Res.*, p. 123990, 2025.

[39] Y. A. Sema, O. E. Urgessa, and A. K. Ayele, “Evaluating rumen fluid-inoculated lignocellulosic substrates for biogas production,” *East African J. Sci.*, vol. 14, no. 2, pp. 99–110, 2020.

[40] L. Li, Q. He, X. Zhao, D. Wu, X. Wang, and X. Peng, “Anaerobic digestion of food waste: Correlation of kinetic parameters with operational conditions and process performance,” *Biochem. Eng. J.*, vol. 130, pp. 1–9, 2018.

Computational and Experimental Research in Materials and Renewable Energy (CERiMRE)
Volume 8, Issue 2, page 175-206
eISSN : 2747-173X

Submitted : September 11, 2025
Accepted : November 12, 2025
Online : November 28, 2025
DOI : 10.19184/cerimre.v8i2.4

[41] A. R. Keshtkar, G. Abolhamd, B. Meyssami, and H. Ghaforian, “Modeling of anaerobic digestion of complex substrates,” 2003.

[42] J. N. Meegoda, B. Li, K. Patel, and L. B. Wang, “A review of the processes, parameters, and optimization of anaerobic digestion,” *Int. J. Environ. Res. Public Health*, vol. 15, no. 10, 2018, doi: 10.3390/ijerph15102224.

[43] T. N. T. M. Marzuki *et al.*, “Enhancement of bioreactor performance using acclimatised seed sludge in anaerobic treatment of chicken slaughterhouse wastewater: Laboratory Achievement, Energy Recovery, and Its Commercial-scale Potential,” *Animals*, vol. 11, no. 11, p. 3313, 2021.

[44] Y. Hu, T. Kobayashi, G. Zhen, C. Shi, and K.-Q. Xu, “Effects of lipid concentration on thermophilic anaerobic co-digestion of food waste and grease waste in a siphon-driven self-agitated anaerobic reactor,” *Biotechnol. Reports*, vol. 19, p. e00269, 2018.

[45] K. Jaman *et al.*, “Anaerobic digestion, codigestion of food waste, and chicken dung: Correlation of kinetic parameters with digester performance and on-farm electrical energy generation potential,” *Fermentation*, vol. 8, no. 1, p. 28, 2022.